Copyright © 2007 by ABCM

COMPARATIVE STUDY OF STRUCTURED AND UNSTRUCTURED MESHES FOR COMPRESSIBLE FLOWS

Gustavo Bono, gbono@mecanica.ufrgs.br
Federal University of Rio Grande do Sul
Mechanical Engineering Postgraduate Program
Av. Sarmento Leite 425, 90050-170 Porto Alegre, RS, Brazil

Armando M. Awruch, amawruch@ufrgs.br
Federal University of Rio Grande do Sul
Applied and Computational Mechanical Center
Av. Osvaldo Aranha 99, 90035-190, Porto Alegre, RS, Brazil

Abstract. *The mesh influence for the solution of compressible flows with two explicit schemes is presented. The investigations measured the order of accuracy, absolute error and the computational cost with structured and unstructured meshes. Two explicit Taylor-Galerkin schemes (one-step and two-step) with a linear tetrahedral and tri-linear hexahedral elements are employed to analyze the fluid flow. Finally, some numerical analyses in inviscid and viscous flows are discussed. This article includes a reflection of an oblique shock and a viscous flow over an airfoil.*

Keywords*: finite element method, compressible flow, structured mesh, unstructured mesh*

1. INTRODUCTION

The rapid growth in the power and availability of computers in recent years has led to the development of many schemes for solving the Euler and Navier-Stokes equations successfully, and as a result numerical simulations are beginning to complement or even replace experimental measurement. In the aerospace industry today Computational Fluid Dynamics (CFD) plays an increasingly important role as a tool for design and analysis.

Computational methods are continuously being required to deliver more accurate solutions for more complex realistic configurations at lower computational cost. Traditionally, structured mesh (quadrilateral or hexahedral elements) approach have been employed to discretize the computational domain. The natural ordering of quadrilateral/hexahedral elements enables the construction of very efficient numerical algorithms for solving the flow equations. While amenable to algorithmic efficiency, structured mesh are inherently difficult for discretizing complex geometries. Unstructured mesh methods originally emerged as a viable alternative to the structured mesh techniques for discretizing complex geometries. In unstructured meshes triangular elements in two dimensions and tetrahedral elements in three-dimensions are used. This not only provides greater flexibility for discretizing complex domains but also enables straightforward implementation of adaptive techniques where node may be added or deleted, while mesh connectivity is updated locally, in order to enhance solution accuracy.

The choice of the type of mesh element to be employed in the aerospace and aeronautical problems depends on the delivered accuracy, efficiency, and flexibility of the numerical solver. A two dimensional study by Aftosmis *et al.* (1994) observed little difference in accuracy between equivalent meshes of quadrilateral and triangular elements. Hexahedral meshes have a better accuracy than the tetrahedral meshes in three dimensional experiments (Baker, 2005).

The time integration, for instance, can be performed in one of the two classical approaches, explicit or implicit techniques. Implicit methods are computationally more expensive, but have less stringent stability bounds. Explicit methods are relatively simple to code and implemented, and are easily cast in a form suitable for efficient parallelization. They require less memory than implicit methods, since only one flow field solution needs to be stored at a time.

In the current work, two explicit Taylor-Galerkin schemes for solving the Euler and Navier-Stokes equations in the context of structured and unstructured meshes are investigated. The present comparison intends to emphasize important features of these numerical schemes and elements. The tests include the reflection of an oblique shock for which there exists a closed-form solution to the compressible Euler equations, as well as the laminar transonic flow past an airfoil.

2. THE GOVERNING EQUATIONS

Let $\Omega \subset R^{n_{sd}}$ and (0,T) be the spatial and temporal domains, respectively, where n_{sd} = 3 is the number of space dimensions, and let Γ denote the boundary of Ω. The spatial and temporal coordinates are denoted by **x** and t. We consider the conservation law form of the Navier-Stokes equations governing unsteady compressible flows with no source terms:

$$\frac{\partial \mathbf{U}}{\partial t}+\frac{\partial \mathbf{F}_i}{\partial x_i}+\frac{\partial \mathbf{G}_i}{\partial x_i}=0 \tag{1}$$

where **U** is the unknown vector of the conservation variables, $\mathbf{F}_i$ and $\mathbf{G}_i$ are, respectively, the inviscid and viscous flux vectors given by

$$\mathbf{U}=\begin{Bmatrix}\rho\\ \rho v_i\\ \rho e\end{Bmatrix},\qquad \mathbf{F}_i=\begin{Bmatrix}\rho v_j\\ \rho v_i v_j+p\,\delta_{ij}\\ v_j\left(\rho e+p\right)\end{Bmatrix},\qquad \mathbf{G}_i=\begin{Bmatrix}0\\ -\tau_{ij}\\ -\tau_{ji}v_i-q_j\end{Bmatrix}, \tag{2}$$

with i, j = 1,2,3. Here v_i is the velocity component in the direction of the coordinate x_i, ρ is the specific mass, p is the thermodynamic pressure, τ_{ij} are the components of the viscous stress tensor, q_j is the heat flux vector, e is the total specific energy and δ_{ij} is the Kronecker delta function.

For a calorically perfect gas, the equation of state and internal energy i are given by the following equations

$$p=\left(\gamma-1\right)\rho\, i,\qquad i=c_v\,T=e-\frac{1}{2}v_i\,v_i \tag{3}$$

where T is the temperature and $\gamma=c_p/c_v$ with c_p and c_v being the specific heat coefficients at constant pressure and constant volume, respectively. The viscous stress tensor τ_{ij} and the heat flux vector q_j are defined as

$$\tau_{ij}=\lambda\, v_{k,k}\,\delta_{ij}+\mu\left(v_{i,j}+v_{j,i}\right),\qquad q_j=-k_{ij}\,T_{,k} \tag{4}$$

where k = 1,2,3. Here k_{ij} represents the components of the conductivity tensor, λ and μ are the volumetric and dynamic viscosity coefficients, respectively. The dynamic viscosity and coefficient of thermal conductivity depend an temperature and therefore are modeled using Sutherland's law (White, 1974)

$$\mu=\left(\frac{T}{T_{ref}}\right)^{3/2}\frac{T_{ref}+S_\mu}{T+S_\mu},\qquad k=\left(\frac{T}{T_{ref}}\right)^{3/2}\frac{T_{ref}+S_k}{T+S_k} \tag{5}$$

where T_{ref} is the temperature reference and S_μ = 110 K and S_k = 194 K for atmospheric air.

Initial and boundary conditions must be added to Eqs. (1)-(2) in order to define uniquely the problem.

3. A TAYLOR-GALERKIN FORMULATION

The numerical scheme is obtained expanding in Taylor series the governing equation and applying after the space discretization process, using the Finite Element Method (FEM) in the context of the classical Bubnov-Galerkin scheme. This approach can be interpreted as the finite element version of the Lax-Wendroff scheme used in finite differences. Two schemes for explicit time integration (one-step and two-step methods) are investigated for solving the compressible inviscid/viscous flow problems.

This temporal integration provides second-order accuracy for time derivative. The formulation exclusively employs tetrahedral and hexahedral finite elements which provide second-order spatial accuracy. Linear unstructured finite elements were chosen because they can be easily generated for complex geometries and exactly integrated without numerical quadrature. To obtain important savings in CPU time and computer memory, an analytical evaluation of the eight node hexahedral element matrices was performed.

3.1. Time discretization: The one-step scheme

The one-step scheme is similar to that presented by Donea (1984). Expanding the conservation variables **U** at $t=t^{n+1}$ in Taylor series including the first and second derivatives, resulting in

$$\Delta\mathbf{U}^{n+1}=\Delta t\left(\frac{\partial \mathbf{U}}{\partial t}\right)^{n+s_1}+\frac{\Delta t^2}{2!}\left(\frac{\partial^2 \mathbf{U}}{\partial t^2}\right)^{n+s_2}+O\left(\Delta t^3\right) \tag{6}$$

with $\Delta\mathbf{U}^{n+1} = \mathbf{U}^{n+1} - \mathbf{U}^{n}$, being s_1 and s_2 the implicitness parameters defined such that

$$\frac{\partial \mathbf{U}^{n+s_1}}{\partial t} = \frac{\partial \mathbf{U}^{n}}{\partial t} + s_1 \frac{\partial \Delta\mathbf{U}^{n+1}}{\partial t} \qquad 0 \le s_1 \le 1 \tag{7}$$

$$\frac{\partial^2 \mathbf{U}^{n+s_2}}{\partial t^2} = \frac{\partial^2 \mathbf{U}^{n}}{\partial t^2} + s_2 \frac{\partial^2 \Delta\mathbf{U}^{n+1}}{\partial t^2} \qquad 0 \le s_2 \le 1 \tag{8}$$

Substituting Eqs. (7) and (8) into Eq. (6), and adopting $s_1 = s_2 = 1/2$, the following expression is obtained

$$\Delta\mathbf{U}^{n+1} = \Delta t\left(\frac{\partial \mathbf{U}^{n}}{\partial t} + \frac{1}{2}\frac{\partial \Delta\mathbf{U}^{n+1}}{\partial t}\right) + \frac{\Delta t^2}{2}\left(\frac{\partial^2 \mathbf{U}^{n}}{\partial t^2} + \frac{1}{2}\frac{\partial^2 \Delta\mathbf{U}^{n+1}}{\partial t^2}\right) \tag{9}$$

Substituting Eq. (1) and its second derivative into Eq. (9), and neglecting high-order terms, we obtain

$$\Delta\mathbf{U}_{I+1}^{n+1} = \Delta t\left[-\frac{\partial \mathbf{F}_i^{\,n}}{\partial x_i} - \frac{\partial \mathbf{G}_i^{\,n}}{\partial x_i} + \frac{\Delta t}{2}\frac{\partial}{\partial x_k}\left(\mathbf{A}_k^{\,n}\frac{\partial \mathbf{F}_i^{\,n}}{\partial x_i}\right)\right] + \frac{\Delta t}{2}\left[-\frac{\partial \Delta\mathbf{F}_{iI}^{\,n+1}}{\partial x_i} - \frac{\partial \Delta\mathbf{G}_{iI}^{\,n+1}}{\partial x_i} + \frac{\Delta t}{2}\frac{\partial}{\partial x_k}\left(\mathbf{A}_k^{\,n}\frac{\partial \Delta\mathbf{F}_{iI}^{\,n+1}}{\partial x_i}\right)\right] \tag{10}$$

where I is an iteration counter, $\mathbf{A}_i$ is the convection Jacobian defined as $\mathbf{A}_i = \partial\mathbf{F}_i/\partial\mathbf{U}$ (Hughes and Tezduyar, 1984), $\Delta\mathbf{F}_i^{n+1} = \mathbf{F}_i^{n+1} - \mathbf{F}_i^{n}$ and $\Delta\mathbf{G}_i^{n+1} = \mathbf{G}_i^{n+1} - \mathbf{G}_i^{n}$.

In expression (10), the variables at time level $n+1$ are involved in the left and right sides of the equation, therefore it is necessary to use an iterative scheme.

3.2. Time discretization: The two-step scheme

The two-step scheme is similar to that presented by Kawahara and Hirano (1983). In the first step, corresponding to the time interval $[t^n, t^{n+1/2}]$, the unknown vector $\mathbf{U}$ at $t = t^{n+1/2}$ is expanded in Taylor series, resulting in

$$\Delta\mathbf{U}^{n+1/2} = \left(\frac{\Delta t}{2}\right)\frac{\partial \mathbf{U}^{n}}{\partial t} + \frac{\left(\Delta t/2\right)^2}{2!}\frac{\partial^2 \mathbf{U}^{n}}{\partial t^2} + O\left(\Delta t^3\right) \tag{11}$$

with $\Delta\mathbf{U}^{n+1/2} = \mathbf{U}^{n+1/2} - \mathbf{U}^{n}$. Substituting Eq. (1) and its second derivative into Eq. (11), and neglecting high-order terms, gives

$$\Delta\mathbf{U}^{n+1/2} = \frac{\Delta t}{2}\left[-\frac{\partial \mathbf{F}_i^{\,n}}{\partial x_i} - \frac{\partial \mathbf{G}_i^{\,n}}{\partial x_i} + \frac{\Delta t}{4}\frac{\partial}{\partial x_i}\left(\mathbf{A}_i^{\,n}\frac{\partial \mathbf{F}_j^{\,n}}{\partial x_j}\right)\right] \tag{12}$$

In the second step, $\mathbf{U}$ at time t^{n+1} is determined by expanding Eq. (1) in Taylor series, obtaining the following expression

$$\Delta\mathbf{U}^{n+1} = \Delta t\left(\frac{\partial \mathbf{U}}{\partial t}\right)^{n} + \frac{\Delta t^2}{2!}\left(\frac{\partial^2 \mathbf{U}}{\partial t^2}\right)^{n} + O\left(\Delta t^3\right) \tag{13}$$

with $\Delta\mathbf{U}^{n+1} = \mathbf{U}^{n+1} - \mathbf{U}^{n}$. Substituting Eq. (1) and its second derivative into Eq. (13), and neglecting high-order terms, the following expression is obtained

$$\Delta\mathbf{U}^{n+1} = \Delta t\left[-\frac{\partial \mathbf{F}_i}{\partial x_i} - \frac{\partial \mathbf{G}_i}{\partial x_i} + \frac{\Delta t}{2}\frac{\partial}{\partial x_i}\left(\mathbf{A}_i\frac{\partial \mathbf{F}_j}{\partial x_j}\right)\right]^{n+\frac{1}{2}} \tag{14}$$

where the convection Jacobian $\mathbf{A}_i$ is defined as $\mathbf{A}_i = \partial \mathbf{F}_i / \partial \mathbf{U}$ (Hughes and Tezduyar, 1984).

3.3. Spatial discretization

Applying the classical Bubnov-Galerkin weighted residual method in the context of the FEM to Eq. (10), for the one-step scheme, and Eqs. (12) and (14), for the two-step scheme, the spatial discretization are obtained. The computational domain was divided into a finite number of tri-linear hexahedral elements (structured mesh) or linear tetrahedral elements (unstructured mesh). The consistent mass matrix is substituted by the lumped mass matrix and then these equations are solved with an explicit scheme.

The proposed schemes are conditionally stable, and the local stability condition for element *E* is given by

$$\Delta t_E = \delta \frac{L_E}{a + \left(v_i \, v_i \right)^{1/2}} \tag{15}$$

where L_E is a characteristic dimension of the element, a is the sound speed and δ is a safety coefficient (in this work the coefficient adopted were $\delta = 0.1$ or 0.3).

In order to stabilize the solution numerically, specially in the presence of strong shocks, it is necessary to add numerical damping to the flow solver. An artificial viscosity model, as proposed by Argyris *et al.* (1989), is used due to its simplicity and efficiency in terms of CPU time. An artificial viscosity is added explicitly to the non-smoothed solution as follows

$$\mathbf{U}_s^{n+1} = \mathbf{U}^{n+1} + \mathbf{M}_L{}^{-1} \mathrm{D} \tag{16}$$

where $\mathbf{M}_L$ is the assembled lumped mass matrix, $\mathbf{U}_s^{n+1}$ and $\mathbf{U}^{n+1}$ are the smoothed and non-smoothed solutions at $t + \Delta t$, respectively. The vector D is given by

$$\mathrm{D} = \sum_{\mathrm{ele}} \mathrm{CFL} \; \mathrm{CAF} \; S_{ele} \left[\mathbf{M} - \mathbf{M}_L \right]_{ele} \mathbf{U}_{ele}^n \tag{17}$$

where *ele* is an index referred to a specific element, $\mathrm{CFL} = \Delta t / \Delta t_E$ is the local Courant-Friedrichs-Lewy number, CAF is an artificial damping coefficient given by the user, S_{ele} is a pressure sensor at element level obtained as an average of nodal values S_i. Values of S_i are components of the following assembled global vector

$$S_{\mathrm{i}} = \sum_{\mathrm{ele}} \frac{\left| \left(\mathbf{M} - \mathbf{M}_L \right)_{ele} \mathbf{p} \right|_i}{\left[\left| \mathbf{M} - \mathbf{M}_L \right|_{ele} \mathbf{p} \right]_i} \tag{18}$$

where **p** is the pressure vector of a specific element, the bars indicate that absolute values of the corresponding terms must be taken and, finally, **M** is the consistent mass matrix at element level.

The constant CAF must be specified with care in order to avoid interferences of artificial and physical viscosities. In this work $0.8 \le \mathrm{CAF} \le 1.0$ were adopted.

4. NUMERICAL EXAMPLES

In this section two examples are presented in order to evaluate the accuracy, the capability and the performance of the two explicit Taylor-Galerkin schemes in the context of structured / unstructured meshes applied to the solution of compressible inviscid and viscous problems.

Finally, it is assumed that the fluid has a specific heat ratio and a constant Prandtl number equal to 1.4 and 0.72, respectively.

4.1. Reflection of an oblique shock in a inviscid flow

The rectangular domain $\{0 \le x \le 4.10, 0 \le y \le 1.0\}$ and boundary conditions of this problem are shown in Fig. 1. Along the inflow ABC all variables are fixed; zero normal velocity is imposed at the wall (AD) and along CD all variables are left free. The exact solution is formed by an incident shock with angle 29 º and a reflected shock with angle 23.28 º. The solution after the second shock is: $\rho = 2.687$; $p = 2.934$; $M = 1.942$; $v_1 = 2.401$ and $v_2 = v_3 = 0$.

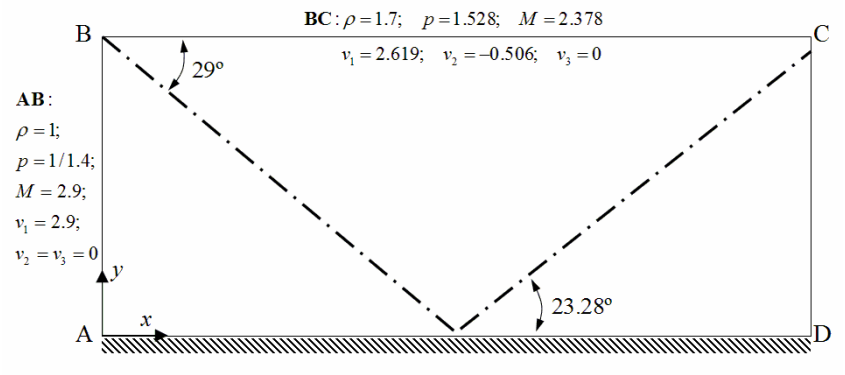

Figure 1. Reflection of an oblique shock and boundary conditions

Four uniform meshes M1, M2, M3 and M4 consisting of $21 \times 11 \times 2$, $41 \times 21 \times 2$, $61 \times 31 \times 2$ and $81 \times 41 \times 2$ nodes, respectively were considered. The meshes with hexahedral elements contains 200, 800, 1800 and 3200 elements and the meshes with tetrahedral 1000, 4000, 9000 and 16000 elements, respectively. The mesh with tetrahedral is obtained by subdividing each hexahedral element into five tetrahedral elements.

In Figure 2 the meshes with hexahedral and tetrahedral elements, respectively, are shown.

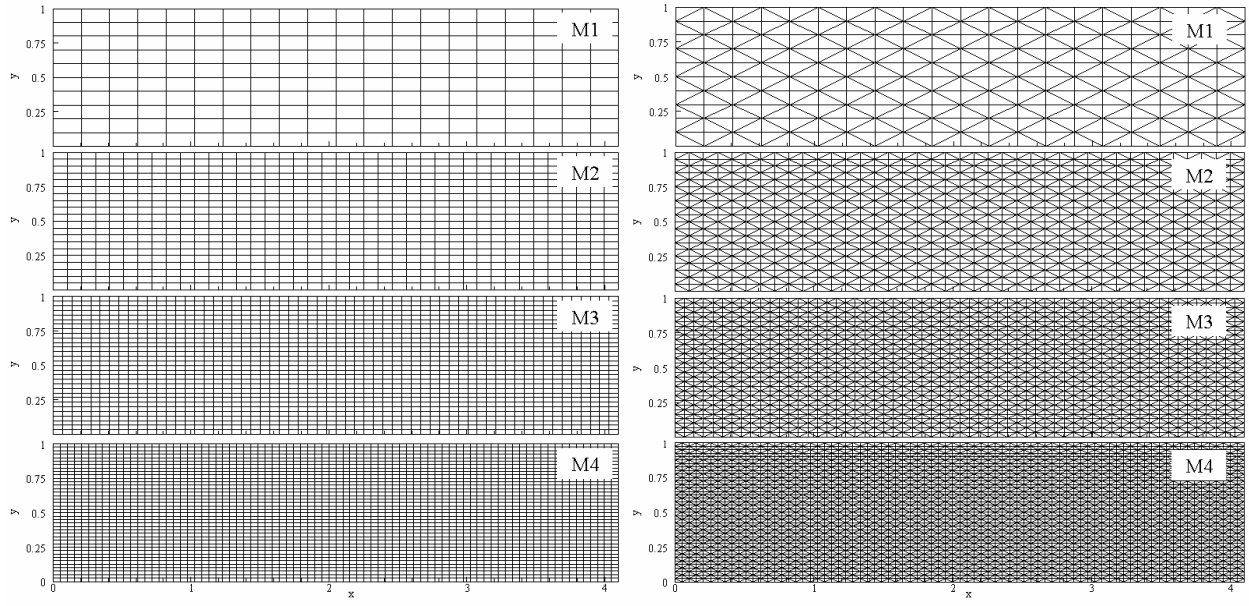

Figure 2. Meshes with hexahedral and tetrahedral elements

Figures 3 and 4 show the specific mass at $y = 0.25$ obtained with the four meshes of hexahedral (H) / tetrahedral (T) elements with the one-step and with the two-step (P2) schemes.

The results for hexahedral meshes exhibit a good agreement with exact solutions and numerical results reported in Shakib *et al.* (1991). A small oscillation in the vicinity of the second shock is observed when tetrahedral meshes are used. Also, these tetrahedral meshes fail to give an exact specific mass behind the second shock. In the mesh M4 only the tetrahedral mesh with one-step scheme overestimate the specific mass.

The accuracy of the numerical solution for the problem is measured by the average error defined in the L_1 norm and the L_2 norm. For specific mass, the two norms are given by

$$L_1 = \frac{1}{nno}\sum_{i=1}^{nno}\left|\frac{\rho_i - \rho_i^e}{\rho_i^e}\right| \qquad \text{and} \qquad L_2 = \sqrt{\frac{1}{nno}\sum_{i=1}^{nno}\left(\frac{\rho_i - \rho_i^e}{\rho_i^e}\right)^2} \tag{19}$$

where ρ^e represents the exact solution while and nno is the number of nodes.

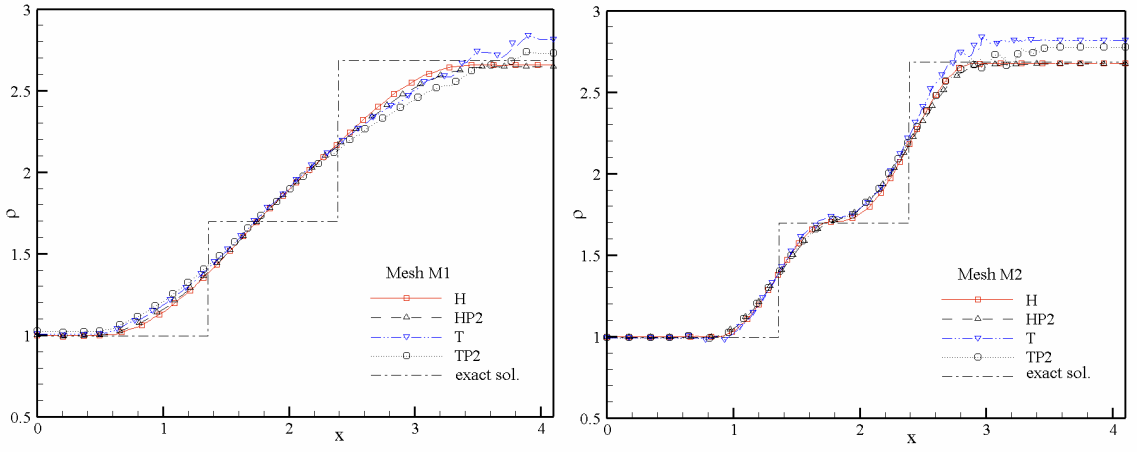

Figure 3. Comparison between exact solution and numerical results of the specific mass along the line $y = 0.25$ for mesh M1 and M2

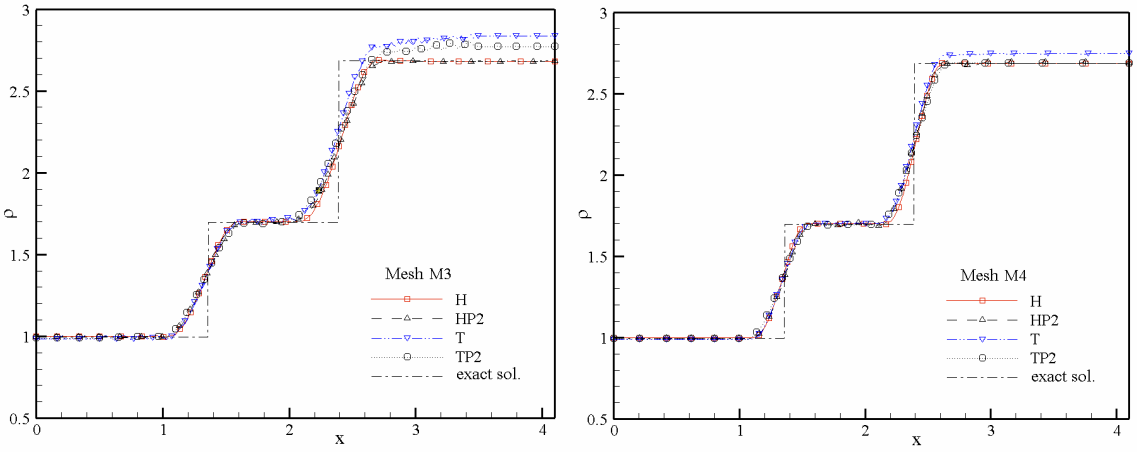

Figure 4. Comparison between exact solution and numerical results of the specific mass along the line $y = 0.25$ for mesh M3 and M4

In the error convergence study, we presents plots of $log\, L_1(\Omega)$ and $log\, L_2(\Omega)$ versus $log(h)$. The results for the specific mass are presented in Fig. 5 for hexahedral / tetrahedral elements with the one-step and the two-step schemes. Analyzing Fig. 5 it is observed that the error decreases as the grid size decreases. The average mesh density h for the hexahedral and tetrahedral meshes is defined as $h = (1/nno)^{1/3}$.

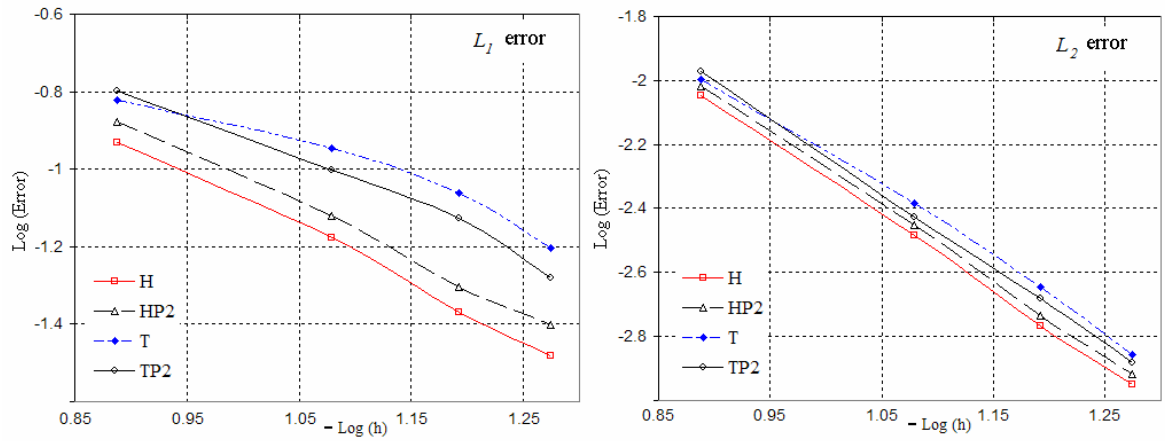

Figure 5. Convergence study for the reflection of an oblique shock problem

In structured meshes a two-step scheme is slightly less accurate than the one-step scheme, while in unstructured meshes a one-step scheme is slightly less accurate than the two-step scheme. Finally, we point out that hexahedral elements have better accuracy than tetrahedral elements. The error is lower for hexahedral elements, independent of the finite element mesh.

The asymptotic convergence rate of errors, given in Table 1, which is measured over the two finest meshes, is just slightly less than 2.0 for $L_1(\Omega)$ norm. Note, however, that the order of convergence is slightly over 2.0 for $L_2(\Omega)$ norm. This is indeed consistent with the second-order accuracy of the spatial discretization that was used.

Table 1. Order of convergence for the example of the reflection of an oblique shock problem.

element / scheme	L_1	L_2
H	1.378	2.257
HP2	1.213	2.241
T	1.715	2.588
TP2	1.907	2.470

4.2. Transonic viscous flow around an airfoil

To investigate these schemes in viscous flows and the influence of different type of elements, the flow around a NACA 0012 airfoil is computed. The flow is specified by $M_\infty = 0.80$, the viscosity by Re = 500 and an angle of attack is equal to 10 deg. With these conditions, a separation bubble extends over more than an half of the upper surface. The airfoil wall is assumed to be adiabatic, and non-slip condition is specified for the velocity on the surface of the airfoil.

Solutions were obtained for three meshes consisting of 19680, 27860 and 40450 nodes, respectively. The meshes with hexahedral elements have 9600, 13600 and 19800 elements meanwhile the meshes with tetrahedral have 48000, 68000 and 99000 elements, respectively. The mesh with tetrahedrals is obtained by subdividing each hexahedral into five tetrahedrals.

A sample of Mach number contours and the streamlines at the mesh with 27860 nodes and 68000 tetrahedrals using the one-step scheme is shown in Fig. 6.

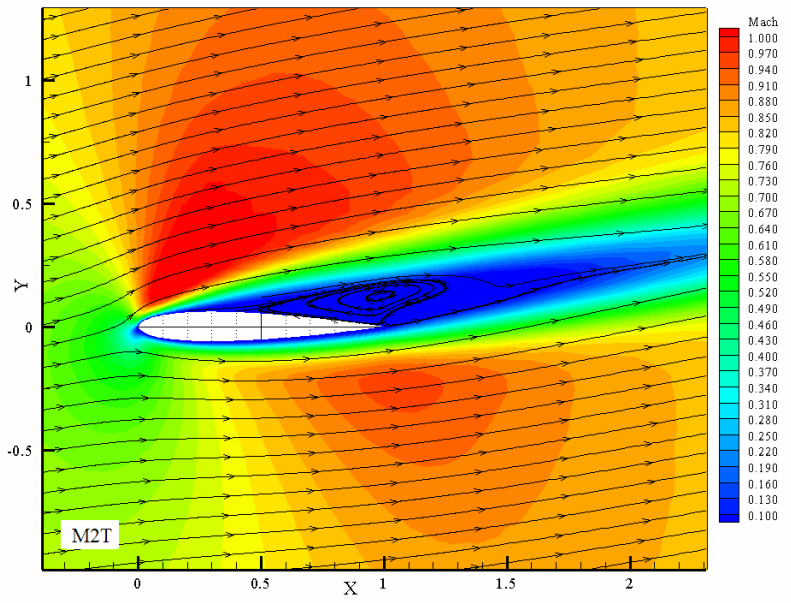

Figure 6. Mach number contours on the mesh with 27860 nodes and 68000 tetrahedral elements for the NACA 0012 airfoil

Contours of pressure for the mesh with 19680 nodes and 9600 hexahedrals using the one-step and two-step schemes are shown in Fig. 7-*a* and Fig. 7-*b*. Both solutions are very similar and agree with those reported in Tang and Hafez (2001). A comparison of the pressure coefficient distributions obtained from the finest meshes with hexahedral and tetrahedral elements using the one-step scheme are plotted in Fig. 8. The results obtained are practically coincident with those reporter by Hafez and Wahba (2007).

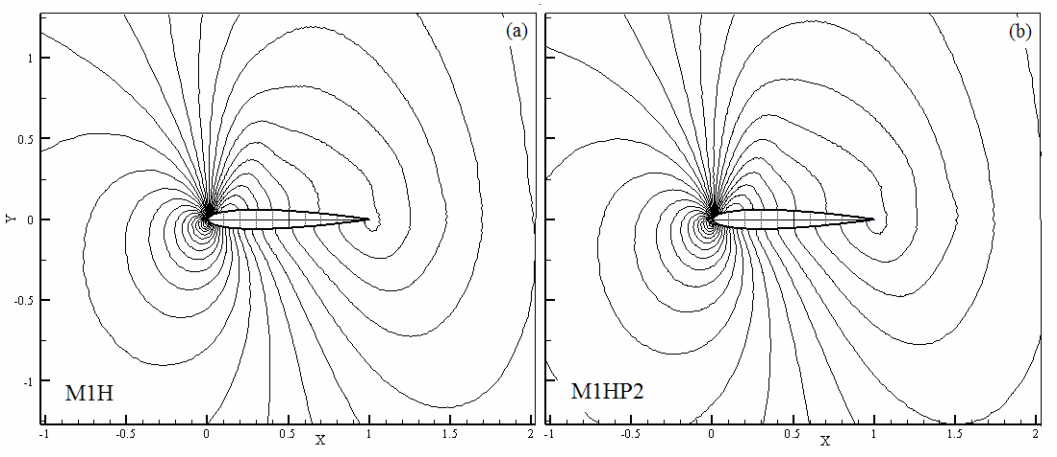

Figure 7. Contours of pressure on the mesh with hexahedral elements for the NACA 0012 airfoil using the one-step and two-step schemes (*a* and *b*, respectively)

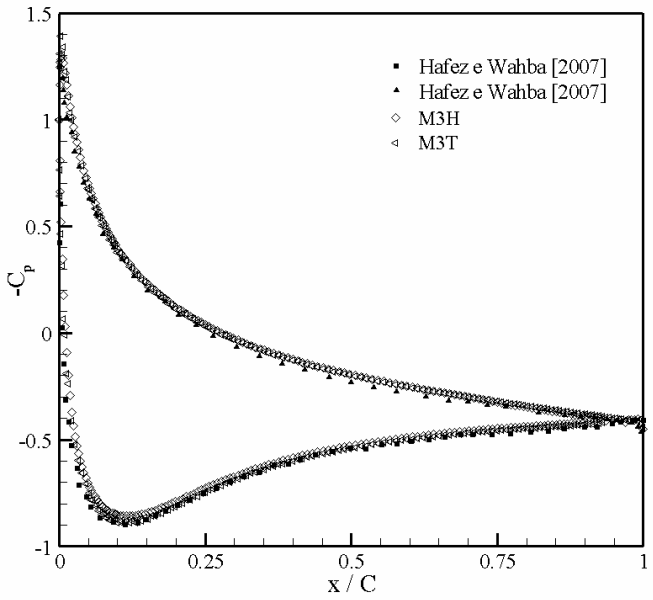

Figure 8. Coefficient of pressure distribution over a NACA 0012 airfoil, compared with result obtained by Hafez and Wahba (2007)

The behavior of the drag and lift coefficients with grid refinement on the hexahedral (H) and tetrahedral (T) meshes and the one-step / two-step (P2) schemes are plotted in Fig. 9, in order to further quantify the accuracy level of the computed pressure distribution.

The drag and lift coefficients obtained by Forsyth and Jiang (1997) ranged between $0.2430 \le C_d \le 0.2868$ and $0.4145 \le C_l \le 0.5170$, respectively. The mesh with tetrahedral elements using the two-step scheme underpredicts the drag and lift coefficients compared with the same meshes using the one-step scheme.

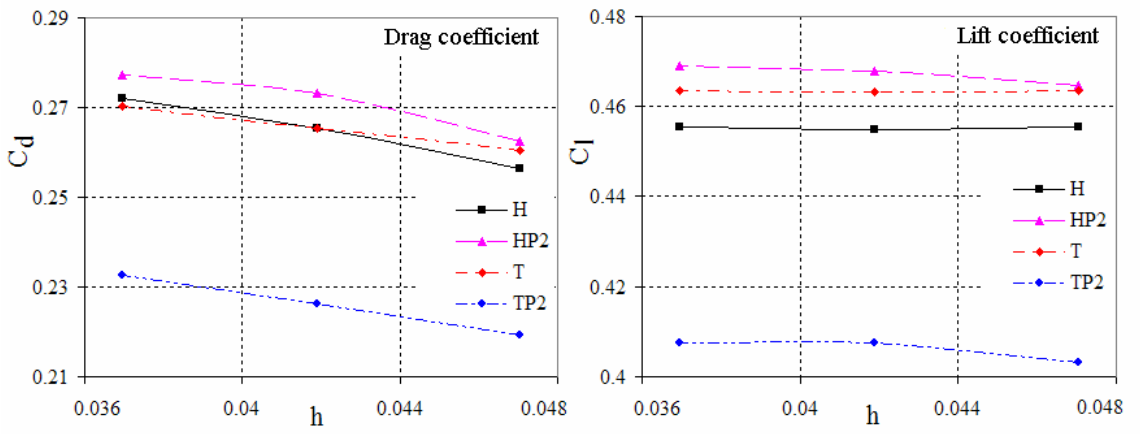

	C_d				C_l			
Mesh	H	HP2	T	TP2	H	HP2	T	TP2
M1	0.2565	0.2625	0.2605	0.2193	0.4554	0.4647	0.4635	0.4032
M2	0.2653	0.2732	0.2653	0.2261	0.4549	0.4678	0.4632	0.4075
M3	0.272	0.2772	0.2704	0.2325	0.4555	0.469	0.4635	0.4076

Figure 9. Variations of the drag and lift coefficients for the transonic viscous flow around a NACA 0012 airfoil

5. CONCLUSION

This paper emphasizes the accuracy and the efficiency of two explicit Taylor-Galerkin schemes in the context of meshes with hexahedral and tetrahedral elements. A comparison among the one-step and two-step scheme using hexahedral and tetrahedral elements leads to the following conclusions: (a) Simulations with meshes employing hexahedral elements, using either the one-step or the two-step scheme, are more accurate and robust in both example studied here, with respect to results employing meshes of tetrahedral elements; (b) In structured meshes a two-step scheme is slightly less accurate than the one-step scheme, while in unstructured meshes a one-step scheme is slightly less accurate than the two-step scheme, for non-viscous flow problem; (c) Simulations with meshes employing tetrahedral elements using the two-step scheme is the most inaccurate in the case of the transonic viscous flow. Clearly, the artificial viscosity plays a fundamental role in the accuracy. The one-step scheme is less diffusive than the two-step scheme allowing to take a smaller value of the coefficient CAF in Eq. (17).

As in the one-step scheme some vectors and matrices are stored to avoid their calculation during the iterative process, the two-step scheme requires less memory (approximately 75 % with respect to the one-step scheme) but it demands more processing time.

In spite of the conclusions given previously, it is necessary to take into account that meshes with tetrahedral elements are more suitable for complex geometries. Another important subject is mesh adaption, which is an essential tool to obtain accurate results in problems involving, for example, strong shock waves, as in the first application (the inviscid flow). Adaptive meshes will be considered in future works.

6. ACKNOWLEDGEMENTS

One of the authors wishes to acknowledge the support of CAPES, through a Doctoral scholarship.

7. REFERENCES

Aftosmis, M., Gaitonde, D. and Tavares, T.S., 1995, ”Behavior of Linear Reconstruction Techniques on Unstructured Meshes”, AIAA Journal, Vol. 33, pp. 2038-2049.

Argyris, J., Doltsinis, I.S. and Friz, H., 1990, ”Study on Computational Reentry Aerodynamics”, Comput. Methods in Appl. Mech. and Engrg., Vol. 81, pp. 257-289.

Baker, T.J., 2005, ”Mesh Generation: Art or Science”, Prog. Aerosp. Science, Vol. 41, pp. 29-63.

Donea, J., 1984, ”A Taylor-Galerkin for Convective Transport Problems”, Inter. J. for Num. Methods in Engrg., Vol. 20, pp. 101-119.

Forsyth, P.A. and Jiang, H., 1997, ”Nonlinear Iteration Methods for High Speed Laminar Compressible Navier-Stokes Equations”, Comput. & Fluids, Vol. 26, pp. 249-268.

Hafez, M. and Wahba, E., 2007, ”Simulations of Viscous Transonic Flows over Lifting Airfoils and Wings”, Comput. & Fluids, Vol. 36, pp. 39-52.

Hughes, T.J.R. and Tezduyar, T.E., 1984, ”Finite Element Methods for First-order Hyperbolic Systems with Particular emphasis on the Compressible Euler Equations”, Comput. Methods in Appl. Mech. and Engrg., Vol. 45, pp. 217-284.
Kawahara, M. and Hirano, H., 1983, ”A Finite Element Method for high Reynods Number Viscous Fluid Flow using two step Explicit Scheme”, Inter. J. for Num. Methods in Fluids, Vol. 3, pp. 137-163.
Shakib, F., Hughes, T.J.R. and Johan, Z., 1991, ”A new Finite Element Formulation for Compressible Fluid Dynamics: X. The Compressible Euler and Navier-Stokes Equations”, Comput. Methods in Appl. Mech. and Engrg., Vol. 89, pp. 141-219.
Tang, C. and Hafez, M., 2001, ”Numerical Simulation of Steady Compressible Flows using a zonal Formulation. Part II: Viscous Flows”, Comput. & Fluids, Vol. 30, pp. 1003-1016.
White, F.W., 1974, ”Viscous Fluid Flow”, McGraw-Hill, New York, USA.

8. RESPONSIBILITY NOTICE

The authors are the only responsible for the printed material included in this paper.